Available online at www.sciencedirect.com
ScienceDirect
Ceramics International 34 (2008) 1959–1964
CERAMICS INTERNATIONAL
www.elsevier.com/locate/ceramint

The effect of silica doping on the microstructure and mechanical properties of c-ZrO_2/SiO_2 composites

S. Tekeli [a,*], T. Boyacıoğlu [b], A. Güral [a]

[a] *Gazi University, Technical Education Faculty, Materials Division, 06500 Teknikokullar, Ankara, Turkey*
[b] *Gazi University, Institute of Science and Technology, 06570 Maltepe, Ankara, Turkey*

Received 25 February 2007; received in revised form 17 April 2007; accepted 14 July 2007
Available online 10 August 2007

Abstract

c-ZrO_2/SiO_2 composites with various amounts of SiO_2 additions were produced by a colloidal processing and pressureless sintering at 1400 °C. The influence of the microstructure and SiO_2 content on the grain size, flexural strength and fracture toughness of the composites were determined. The results showed that SiO_2 had very limited solubility of 0.3 wt% in c-ZrO_2 matrix. This suggests that only small part of the SiO_2 dissolved in the c-ZrO_2 matrix and the rest of SiO_2 segregated at grain boundaries and multiple junctions as amorphous glassy phase. This glassy phase formed rounded grains and prevented the grain growth by minimizing grain boundary energy and mobility. c-ZrO_2/SiO_2 composites having different SiO_2 contents showed high flexural strength and fracture toughness. With the increase of SiO_2 content from 0 to 10 wt%, the grain size, flexural strength and fracture toughness changed from 5.7 to 0.5 μm, 275 to 292 MPa and 1.5 to 3.64 MPa $m^{1/2}$, respectively. The increase in fracture toughness and flexural strength could be attributed to smaller grain size and crack deflection.

Keywords: Cubic zirconia; Silica; Fracture toughness; Flexural strength

1. Introduction

Yttria-stabilized zirconia could be tetragonal or cubic. At room temperature, 3 mol% yttria stabilized zirconia (t-ZrO_2) is tetragonal under certain conditions, whereas 8 mol% yttria stabilized zirconia (c-ZrO_2) is cubic [1]. These two kinds of zirconias are of rather different properties and application aspects. Tetragonal zirconia ceramics has excellent room temperature mechanical properties, such as fracture toughness and flexural strength, caused by a transformation toughening [2,3]. The most important parameter for this toughening mechanism is the grain size. For good mechanical properties, the grain size must be kept below a certain value which is typically in the order of 1 μm for tetragonal zirconia. It is well known that the grain growth in tetragonal zirconia is extremely sluggish both under static and dynamic conditions. Although the crystal structure of cubic zirconia is close to that of tetragonal zirconia, room temperature mechanical properties for cubic zirconia is limited because of thermal stresses, mechanical stresses during operation and lack of transformation toughening. It was reported that [4] the grain growth of cubic zirconia is 20–250 times faster than that of tetragonal zirconia under the same heat treatment conditions.

The cubic structure of zirconia can be stabilized at room temperature by the addition of Y_2O_3 in solid solution. Cubic zirconia is used as a solid electrolyte in solid oxide fuel cells (SOFC) due to its excellent stability and high oxygen ionic conductivity over wide range of oxygen partial pressures [5]. For SOFC applications, good mechanical and chemical stability are required at the high operating temperatures. Poor mechanical properties may cause the cubic zirconia fracture during operations. Therefore, it is necessary to improve the mechanical properties of cubic zirconia. In most ceramics, intergranular amorphous phases exist due to the deliberate addition of sintering aids or impurities from the processing. The presence of these intergranular amorphous phases profoundly influences the fabrication and properties of the materials even when they are used in only trace amount. Silica, which forms an intergranular amorphous phase at sintering and deformation temperatures, can be given as an example of such dopants.

* Corresponding author. Tel.: +90 312 4399760; fax: +90 312 2120059.
E-mail address: stekeli@gazi.edu.tr (S. Tekeli).

0272-8842/$34.00
doi:10.1016/j.ceramint.2007.07.003

Although silica addition has been used for some times to improve densification and superplastic deformation of cubic zirconia [6,7], there is limited information about the effect of silica on the room temperature mechanical properties of cubic zirconia. Therefore, in the present study, the effect of Silica with various amounts on the microstructure, flexural strength and fracture toughness of cubic zirconia was investigated.

2. Experimental procedure

c-ZrO_2/SiO_2 composites containing up to 10 wt% SiO_2 were produced from the commercial powders: 8 mol% yttria-stabilized cubic zirconia (c-ZrO_2) powder, Tosoh, Japan and colloidal silica from Nissan Chemical Industry Co. Ltd., Japan. The average particle sizes were 30 nm for c-ZrO_2 and about 10–20 nm for colloidal silica. The chemical composition of c-ZrO_2 was 13.6 wt% Y_2O_3 (equivalent to 8 mol%), 85.9 wt% ZrO_2 and the following impurities (in wt%), Al_2O_3 0.25, SiO_2 0.10, TiO_2 0.12, Fe_2O_3 0.003, Na_2O 0.002 and CaO 0.02. A colloidal processing was used for the preparation of specimens for fracture toughness and flexural strength measurements. The slurry was prepared by dispersing the designated amount of c-ZrO_2 powder and colloidal silica in ethanol. The slurry was then ball milled for 24 h to obtain a good dispersion and to break-up agglomerates in a plastic container using zirconia balls. The mixed composite powders were dried in argon, sieved through an 60 μm sieve and die-pressed into disks and bars by uniaxial pressing at 30 MPa in a steel die followed by cold isostatic pressing (CIP) at 100 MPa in a rubber tube. For lubrication, the interior surface of the dies was coated with a layer of stearic acid. The specimens were sintered at 1400 °C for 1 h. After sintering, the specimens were sectioned, ground, polished to 1 μm surface finish and finally thermally etched in air for 30 min. at a temperature 50 °C lower than sintering temperature. Scanning electron microscopy (SEM) equipped with an energy dispersive X-ray spectrometer (EDS) attachment was used to characterize the microstructure of as-sintered specimens. The average grain size of the zirconia grains was determined from SEM images of randomly selected areas of the polished and thermally etched specimens using the mean linear intercept method. The average value was obtained based on the analysis of at least 1000 grains for each material.

The flexural strength (σ_f) was measured by three-point bending test at ambient room temperature and calculated by the following equation;

$$\sigma_f = \frac{PL}{2WT^2} \quad (1)$$

where σ_f is flexural strength, P the load, L the span length, W the width of the specimen and T is the thickness of the specimen. The dimension of the bar specimen after polishing to a 3 μm diamond finish was 3 mm high, 4 mm wide and 45 mm long. The specimens were tested by using universal testing machine (Shimadzu). The span length was 30 mm and the crosshead speed was 0.5 mm/min. Before testing the edges of the specimens undergoing tensile stresses were beveled at 45° to avoid the fracture from the specimen edges. A minimum of five specimens was tested in order to establish average values of flexural strength.

For fracture toughness, disk specimens were employed. The dimension of the disk specimen after polishing to a 1 μm diamond finish was 15 mm in diameter and 10 mm in thickness. The fracture toughness was determined by the indentation technique using a Vickers indenter with a load of 20 kg at ambient room temperature. Polished specimens were indented at 10 different locations. Before indentation, a drop of oil was deposited onto the surface of the specimens to minimize moisture-enhanced crack growth. The size of the cracks emanating the indentation centre was measured. Measurements were performed immediately after each indentation in order to avoid any difference in crack length due to the environmental variables such as moisture and time. The indentation fracture toughness was calculated using the formula proposed by Anstis et.al. [8] (half-penny crack);

$$K_{IC} = 0.0016\left(\frac{E}{H_v}\right)^{1/2}\left(\frac{P}{C^{3/2}}\right) \quad (2)$$

where K_{IC} is fracture toughness, E the Young's modulus, H_v the Vickers hardness, P the load and C is the crack length.

3. Results and discussion

Colloidal processing was used for the mixing of powders in order to achieve a uniform distribution and homogeneous microstructure. A major problem in the processing of nano-sized powders is existence of agglomerates which occur spontaneously due to van der Waals forces. While small interparticle pores are easily closed during sintering, large interagglomerate pores need a high sintering temperature or long sintering times to be eliminated. Pores exceeding a critical size even grow during sintering. Hence significant grain growth takes place. To achieve better mechanical behaviour, fine grain size, homogeneous microstructure and high density are necessary. Colloidal processing helps to prevent the agglomeration of fine particles and allows the particle dispersion to be controlled during powder processing. In the present study, the agglomerates which often shrink away from the surrounding powder matrix during sintering causing crack-like voids, responsible for early fracture and leaving big pores in the microstructure after sintering were eliminated by colloidal processing.

The earlier XRD analysis showed that only cubic fluorite structure is the crystalline phase present in both pure c-ZrO_2 and in c-ZrO_2/SiO_2 composites and there were no diffraction peaks of second phases for all compositions. XRD results also indicated that SiO_2 had very limited solubility of ~0.3 wt% into c-ZrO_2 [9,10]. As the solubility limit of SiO_2 in c-ZrO_2 is ~0.3 wt%, SiO_2 can hardly form a solid solution with c-ZrO_2. Therefore, SiO_2 mostly segregated around the c-ZrO_2 grains and at grain boundaries.

Fig. 1 shows representative microstructures of the ZrO_2/SiO_2 composites with various SiO_2 contents. The grains of the undoped c-ZrO_2 were faceted and straight grain boundaries were often seen (Fig. 1a). The grains in the c-ZrO_2/SiO_2

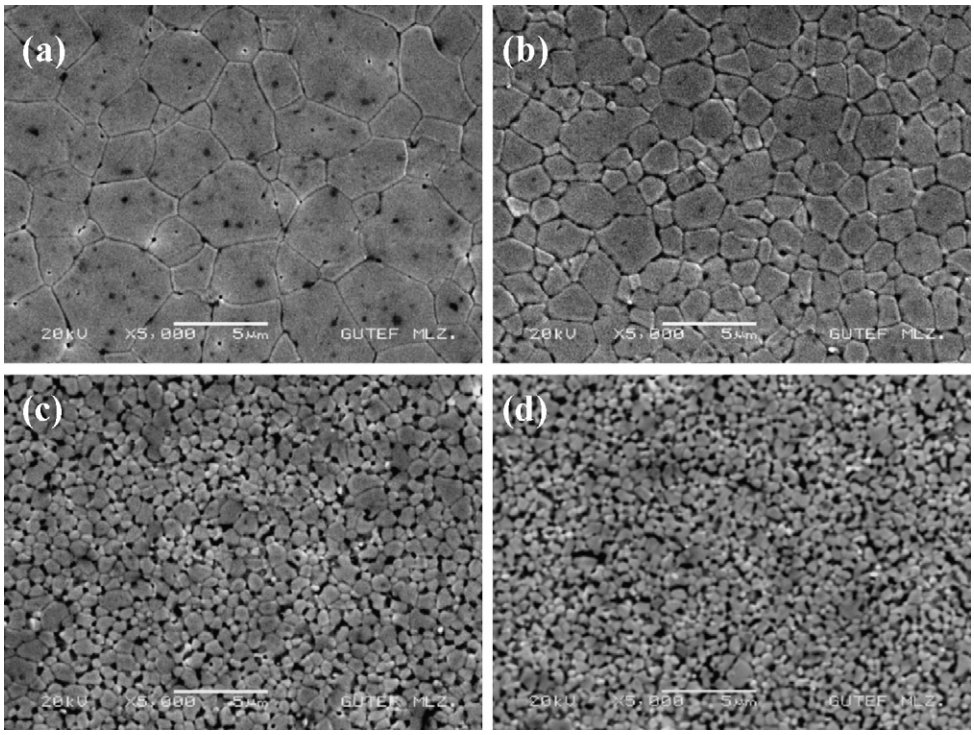

Fig. 1. Microstructures of the c-ZrO_2/SiO_2 composites doped with various amounts of SiO_2 (a) undoped, (b) 1 wt% SiO_2, (c) 5 wt% SiO_2 and (d) 10 wt% SiO_2.

composites were rounded and a darker phase was located along the grain boundaries and at grain boundary triple points (Fig. 1b–d). EDS analyses showed that the darker phase is an amorphous glassy phase enriched with Si. The change in the microstructure with the addition of the SiO_2 can be explained as follows. For a small amount of the SiO_2 addition, less than 0.3 wt%, the SiO_2 dissolves in the c-ZrO_2 lattices so that no amorphous phase is found. For a further increase in the SiO_2 addition, the c-ZrO_2 matrix is saturated with SiO_2 and hence the excess amount of the SiO_2 is preferentially segregated along the grain boundaries and at multiple grain junctions as glass pocket. This glassy phase wets the c-ZrO_2 grains and forms rounded grains. The thickness of this glassy phase increases with increasing SiO_2 content, and the rounded grains are formed due to minimizing interfacial energy between glass and c-ZrO_2 grains. The comparison of the grain size of the specimens at the same heat treatment indicated that grains were larger in the undoped c-ZrO_2 than in the c-ZrO_2/SiO_2 composites. Also, the grain size decreased with increasing SiO_2 content (Fig. 2). To inhibit the grain growth, the grain boundary mobility and energy should be reduced, for example, by impurities, dopants or particles of a second phase. In polycrystalline materials, it has been shown that particles of a second phase with limited solubility are especially effective in pinning grain boundaries and thus minimizing static and dynamic grain growth [11]. The grain boundary mobility decreases with increasing the grain boundary width. Additives and dopants that increase grain boundary width may be effective in minimizing grain growth. Also, the additives that decrease grain boundary energy have an additional effect on minimizing grain growth. A reduction in grain boundary energy occurs when intergranular phases wet the grain boundaries. In the present study, the addition of SiO_2 to the c-ZrO_2 resulted in limiting grain growth by segregation of solute cations to grain boundaries and by wetting the grain boundary at high temperature. The SiO_2 has a higher viscosity and a lower diffusivity at high temperatures. Hence, the grain growth was limited by Zenner pinning of the grain boundaries and by reducing the driving force for grain growth in the presence of the lower energy liquid/ceramic interface. In addition, the grain boundary mobility with respect to grain growth decreased by increasing the effective grain boundary width, as liquid phase distributed along the grain boundaries.

The flexural strength as a function of the SiO_2 content for the c-ZrO_2/SiO_2 composites is shown in Fig. 3. It was seen that the addition of SiO_2 slightly increased the flexural strength of the c-ZrO_2/SiO_2 composites. The improvement in the flexural

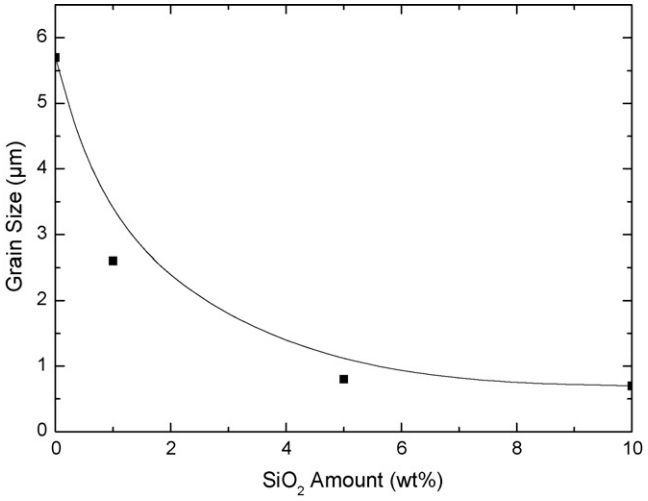

Fig. 2. Grain size variation with SiO_2 content.

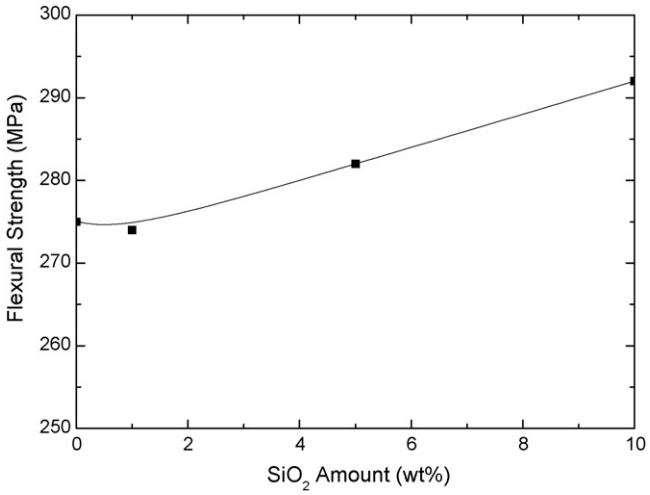

Fig. 3. The effect of SiO_2 content on flexural strength of c-ZrO_2/SiO_2 composites.

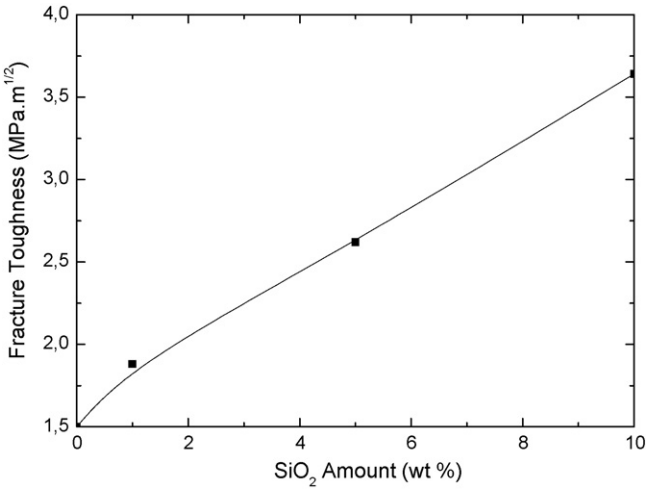

Fig. 4. The effect of SiO_2 addition on fracture toughness of c-ZrO_2/SiO_2 composites.

strength can be attributed to the following reasons. The first is refinement of the matrix grains. As can be seen in Fig. 2 that mean grain size of monolithic c-ZrO_2 sintered at 1400 C was 5.7 μm, while the grain size of the c-ZrO_2/SiO_2 composites containing 1, 5 and 10 wt% SiO_2, sintered at the same sintering temperature were 2.6, 0.8 and 0.7 μm, respectively. The second is the different expansion coefficients of c-ZrO_2 and SiO_2.

The relation between fracture toughness and the SiO_2 content is given in Fig. 4. It is observed that the fracture toughness values increased as the SiO_2 content increased. Fig. 5 shows SEM micrographs of the cracks generated by the indentation load of 20 kg. Note that cracks emanate from the corners of the indents and crack lengths were different depending on the SiO_2 content. For the monolithic c-ZrO_2, the indents with long crack lengths were observed. On the contrary, with increasing SiO_2 amount, the crack lengths were decreased (Fig. 6). The increase in the fracture toughness and the decrease in crack length in the specimens with higher amount of SiO_2 could be attributed to existence of glassy phase and thus smaller grain size. In general, smaller grain size shows higher fracture toughness. When a crack propagates, it follows either the grain boundaries or around grains. The new surfaces are generated with the refinement of grains. This results in greater surface energy and higher value of fracture toughness. Thus, by controlling the grain size, fracture toughness can be controlled. The increase in fracture toughness with increasing SiO_2 content can also be explained in term of the crack propagation. SEM investigations of the indentation cracks on

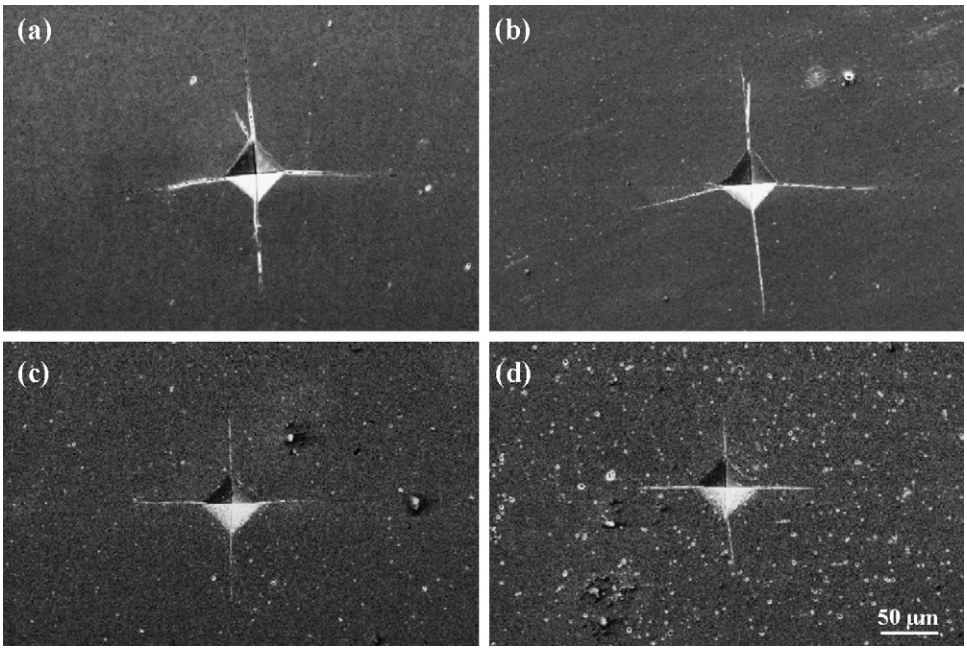

Fig. 5. SEM micrographs of Vickers indentations with different crack lengths in the c-ZrO_2/SiO_2 composites doped with various amounts of SiO_2 (a) undoped, (b) 1 wt% SiO_2, (c) 5 wt% SiO_2 and (d) 10 wt% SiO_2.

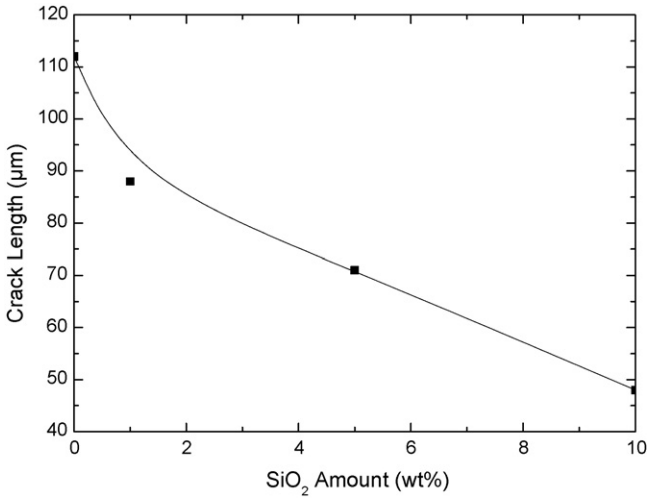

Fig. 6. Evolution of the indentation-crack length as a function of SiO_2 content.

thermally etched surfaces showed that cracks propagated intergranularly as well as transgranularly in the undoped c-ZrO_2 and in the c-ZrO_2/SiO_2 composites (Fig. 7). As shown in Fig. 7, the cracks propagated through the c-ZrO_2 grains, c-ZrO_2 grain boundaries, the interface between the c-ZrO_2 grain and the glassy phase and glass phase depending on the SiO_2 content in the c-ZrO_2/SiO_2 composite. While transgranular crack propagation is dominant in the undoped c-ZrO_2 (Fig. 7 a), the cracks propagated intergranularly in the c-ZrO_2/SiO_2 composites (Fig. 7 b–d). The reason for the intergranular crack propagation was that the c-ZrO_2 grain boundaries and the c-ZrO_2/glassy phase interfaces act as site for crack deflection resulting in non-planar cracks [12]. Generally, it is believed that the glassy phase forms a weaker secondary phase network in the materials; the present results showed that the presence of glassy grain boundary phase did not weaken the grain boundaries and became the preferred crack propagation path in the composites. Another factor that may cause the intergranular crack propagation is the presence of residual stresses in the c-ZrO_2/SiO_2 composites due to different Young's modulus and the coefficients of the thermal expansion between c-ZrO_2 grain ($10.5 \times 10^{-6}\ K^{-1}$) and glassy phase ($0.5 \times 10^{-6}\ K^{-1}$) [13].

4. Conclusions

1) The comparison of the grain size of the specimens indicated that grains were larger in the pure c-ZrO_2 than in the c-ZrO_2/SiO_2 composites. Also, the grain size decreased with increasing SiO_2 content. The addition of second phase silica to the c-ZrO_2 inhibited the grain growth.
2) The flexural strength slightly increased with increasing SiO_2 addition and content. The increase of flexural strength can be attributed to smaller grain size and the different expansion coefficients of c-ZrO_2 and SiO_2.
3) The fracture toughness values increased as the SiO_2 content increased. The crack lengths decreased with increasing SiO_2 content. The increase in fracture toughness and the decrease in crack length in the specimens with higher amount of SiO_2 could be attributed to existence of glassy phase and thus smaller grain size.

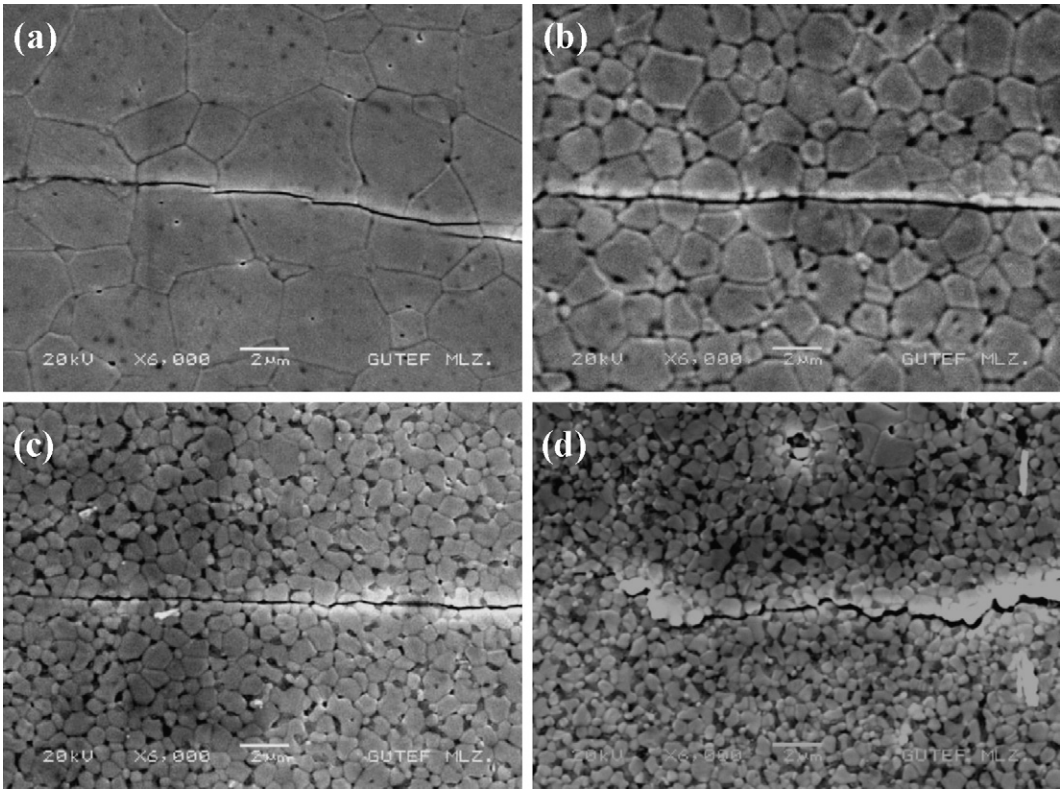

Fig. 7. Crack propagation paths in the c-ZrO_2/SiO_2 composites doped with various amounts of SiO_2 (a) undoped, (b) 1 wt% SiO_2, (c) 5 wt% SiO_2 and (d) 10 wt% SiO_2

Acknowledgements

This work has been supported by DPT (the State Planning Organization of Turkey) under project number 2003K120470. The authors are grateful to the DPT for financial support and Gazi University for the provision of laboratory facilities.

References

[1] J.L. Shi, M.L. Ruan, T.S. Yen, Ceram. Int. 22 (1996) 137–142.
[2] J.Sun, G.Huang, J.Wang, H.Liu, Mater. Sci. Eng. A, in press.
[3] J.A. Allemann, B. Michel, H.B. Marki, L.J. Gauckler, E.M. Moser, J. Eur. Ceram. Soc. 15 (1995) 951–958.
[4] I.G. Lee, I.W. Chen, Sintering 87, in: S. Somiya, M. Yashimura, R. Watanabe (Eds.), Proceedings of the Fourth International Symposium on Science and Technology og Sintering, vol. 2, Elsevier, London, 1988, pp. 340–345.
[5] N.Q. Minh, Ceramic Fuel-Cells, J. Am. Ceram. Soc. 76 (3) (1993) 563–588.
[6] A.A. Sharif, M.L. Mecartney, Acta Mater. 51 (2003) 1633–1639.
[7] A.A. Sharif, P.H. Imamura, T.E. Michell, M.L. Mecartney, Acta Mater. 46 (1998) 3863–3872.
[8] G.R. Anstis, P. Chantikul, B.R. Lawn, D.B. Marshall, J. Am. Ceram. Soc. 64 (1981) 533–543.
[9] S. Tekeli, M. Guru, Key Eng. Mater. vols. 336–338 (2007) 2418–2421.
[10] S.Tekeli, M.Guru, Ceram. Int., in press.
[11] A. Sturm, U. Betz, U. Scipione, H. Hahn, Nanostruct. Mater. 11 (5) (1999) 651–661.
[12] K. Hiraga, K. Morita, B.-N. Kim, Y. Sakka, Mater. Trans. 45 (12) (2004) 3324–3329.
[13] N.-H. Kwon, G.-H. Kim, H.S. Song, H.-L. Lee, Mater. Sci. Eng. A299 (2001) 185–194.